PRAMANA
— journal of
physics

© Indian Academy of Sciences

Vol. 82, No. 1
January 2014
pp. 97–109

Ultrashort laser pulse–matter interaction: Implications for high energy materials

S VENUGOPAL RAO
Advanced Centre of Research in High Energy Materials (ACRHEM), University of Hyderabad, Gachibowli, Hyderabad 500,046, India
E-mail: svrsp@uohyd.ernet.in; soma_venu@yahoo.com

DOI: 10.1007/s12043-013-0647-8; ***e*Publication:** 5 January 2014

Abstract. The interaction of ultrashort [nanosecond (ns)/picosecond (ps)/femtosecond (fs)] pulses with materials is an exhaustive area of research with underlying, and often extremely rich, physics along with a plethora of applications evolving from it. High-energy materials (HEMs) are chemical compounds or mixture of compounds which, under suitable initiation, undergoes a very rapid exothermic and self-propagating decomposition. Herein, we describe the interaction of laser pulses with materials and its implications for studies on HEMs in four parts: (a) ns and fs laser-induced breakdown spectroscopic (LIBS) studies of HEMs towards understanding the molecular dynamics and discrimination, (b) ps/fs pulses interaction with metallic solids towards the production of nanoparticles, nanostructures and their utility in identifying explosive molecules using surface-enhanced Raman scattering studies, (c) interaction of laser pulses with the bulk and surface of glasses and polymers producing micro- and nanostructures for microfluidic/lab-on-a-chip applications, and (d) ultrafast spectroscopic studies for comprehending the excited state dynamics towards elucidation of vibrational dynamics in HEMs. Several applications resulting from these interactions will be discussed in detail.

Keywords. Ultrashort laser pulses; laser-induced breakdown spectroscopy; ablation; laser direct writing; pump–probe technique; high-energy materials.

PACS Nos 82.53.Uv; 42.62.Fi; 52.50.Jm; 52.38.−r; 79.20.Eb; 52.38.Mf

1. Introduction

With the advent of compact ultrafast laser oscillators [1], high-power laser amplifiers [2,3], and other widely tunable radiation sources (ranging from deep ultraviolet to mid- and far-infrared wavelengths) in the last two decades, the research field of ultrafast laser–matter interaction has burgeoned. Depending on the laser pulse duration [nanosecond

(ns), picosecond (ps), femtosecond (fs) or attosecond], energy/intensity, wavelength, and repetition rate the interaction with matter is entirely diverse in different regimes [4,5]. With fs pulses, absorption (ionization) is usually followed by hydrodynamics. However, in the ns regime both absorption and hydrodynamics are coupled. The ramifications of such interactions are farfetched in a variety of fields including control of chemical reactions, nanosurgery using fs pulses, dielectric breakdown, terahertz generation etc. amongst many others [6–9]. High-energy materials (HEMs) are materials that store a huge amount of chemical energy, a majority of which gets converted into mechanical energy during decomposition. Ignition processes such as sparks, shocks, and heat can initiate decomposition of these materials through their excited electronic states [10–13]. Several experimental and theoretical works have demonstrated the importance of excited electronic state decomposition in the energy conversion process. This decomposition is a very complicated mechanism and various laser-based studies have been initiated in the last couple of decades. A complete understanding of the mechanisms responsible for the decomposition of energetic materials from excited electronic states is a requisite for developing novel molecules with higher potential in terms of energy released and their stability [10]. Shock-induced chemistry during the first few picoseconds of even the basic HEMs has been limited to simulations only [14] and there have been very few experimental reports on the vibrational dynamics (useful in understanding the decomposition pathways, for example in simple HEM such as nitromethane) and the dynamics of shock-compressed materials [15–18].

Furthermore, discrimination/classification (and isolation in some cases) of potentially hazardous materials is essential for several civilian (e.g. airport screening) and defense (e.g. detection of land mines) applications. Our research group at Advanced Centre of Research in High Energy Materials (ACRHEM) has focussed our research on laser–matter interaction, especially towards understanding HEMs, for the last six years and herein we present some of our recent results emanating from these studies. The laser–matter interaction with ns, ps, and fs pulses is being pursued extensively and representative results from each of these studies are briefly presented herein. The work, categorized into four parts, is presented as follows: (a) ns- and fs laser-induced breakdown spectroscopic (LIBS) studies, (b) ps and fs ablation studies of plasmonic metals, (c) fs laser direct writing (LDW) studies in polymers, glasses etc., and (d) ps and fs pump–probe studies of novel organic moieties.

1.1 *Ns and fs LIBS studies*

We utilized short pulses (ns and fs) to create optical breakdown on material surfaces to study the light emission to devise mechanisms for identifying/classifying HEMs (e.g. RDX, HMX, pyrazoles) [19–25]. Several laser-based techniques have recently been developed to identify hazardous compounds. Amongst them LIBS has been identified as an attractive, versatile technique with many encouraging attributes such as stand-off detection capability, trace material detection, and high speed [26,27]. Civis *et al* [28] utilized LIBS technique along with selected ion flow tube mass spectrometry for studying the electronic bands of CN (388 nm), OH (308.4 nm), and NO (237.1 nm) radicals of a FOX-7 molecule and they could construct a reaction scheme of the early phases of explosive decomposition.

1.2 *Ps and fs ablation studies*

Metallic samples (Ag, Al, Cu), when exposed to focussed ultrashort laser pulses (ps and fs), produced uniformly distributed nanoparticles (NPs) in solutions (such as acetone, chloroform, water etc.) and nanostructures (NSs) on the surface [29–33]. Both the colloids (NPs) and NSs can be utilized for ultralow concentration detection of explosives/HEMs using surface-enhanced Raman scattering (SERS) technique.

1.3 *fs LDW studies*

We have investigated the modifications within and on the surface of the bulk transparent dielectrics (e.g. glasses) and polymers when exposed to tightly focussed (high NA) ∼100 fs pulses using laser direct writing (LDW) technique. LDW [34] is a ubiquitous technique due to the relative ease of fabricating microstructures and nanostructures combined with the possibility of integration for realizing complex, truly three-dimensional devices. Such developed structures in polymers, glasses, and HEMs [35–46] form building blocks for lab-on-a-chip devices useful in the fields of security and sensing. We can envisage point-of-care diagnostics for explosives detection using disposable, hand-held devices.

1.4 *Excited state dynamics using fs/ps pulses*

The interaction of short pulses (ps and fs) with organic materials and semiconductors was utilized for studying the ps and fs excited state dynamics along with their third-order optical nonlinearities [47–64]. Multiphoton excitation leads the population to high lying excited states and a delayed ultrafast probe can resolve the lifetimes of electronic states and the vibrational cooling dynamics. Novel molecules such as phthalocyanines, porphycenes, and corroles along with semi-insulating and low-temperature grown GaAs (useful for generating terahertz radiation) were investigated using ps/fs degenerate pump–probe techniques.

2. Results and discussion

2.1 *Ns and fs LIBS studies*

Fs laser plasma can be produced with lower incident laser energy and ablation threshold compared to the ns case. Furthermore, the produced plasma emits nearly a backgroundless continuum. In comparison to ns LIBS, fs laser-produced plasma has negligible interaction with the input pulses. This means that most of the pulse energy is utilized in creating plasma resulting in small, deep crater formation and thereby precise, smooth structures in solid targets. Materials such as plastics, organic explosives, and also a few bacterial samples possessing composition of the type '$C_\alpha H_\beta N_\gamma O_\delta$' exhibit similar molecular and elemental signatures in their LIBS spectra. These molecular peaks are important and are used widely for classifying these materials amongst others. There are three major possibilities ([21,22] and references therein) which give rise to the CN formation in plasma: (a) Direct evaporation of molecular radicals present in the sample, (b)

due to the secondary reactions occurring between C, N, and C_2 present in the plasma, (c) reaction between C, C_2 from the plasma with atmospheric nitrogen. We investigated the molecular features of LIBS spectra recorded for NTO, RDX, and TNT samples in three environments, viz. air, nitrogen, and argon with fs laser pulses. Plasma chemistry involves the formation of molecular fragments which is a complex phenomenon. The surroundings of plasma influence the molecular formation significantly. Therefore, it is necessary to study the sources for the formation of CN and C_2 molecules, since this data could be important for classification. We had chosen three different atmospheres such that, one was nitrogen which created 100% nitrogen surrounding the plasma, second was in ambient air atmosphere where more than 75% of nitrogen was available. In the last set we performed experiments in argon buffer gas (0% nitrogen) which was used to create inert atmosphere surrounding the plasma for demonstrating a situation for CN formation between the atoms present in the plasma only. We attempt to understand the CN molecular formation mechanism and figure out the contribution from the surrounding atmosphere to the plasma.

Nanosecond LIBS studies were performed on ammonium perchlorate (AP), ammonium nitrate (AN), and boron potassium nitrate (BPN) to evaluate the prospects of non-gated collection scheme against the gated light collection scheme [19]. O/N ratios have been calculated from the LIBS spectra. In the case of gated spectrometer data of AP, all the three O/N ratios demonstrated a good agreement with the actual stoichiometric (O/N) ratio while for BPN two of the O/N ratios matched with the actual values. We observed that for the spectra recorded >1000 ns, the calculated O/N ratios were in good concurrence with the actual stoichiometry values. In the non-gated scheme, the calculated O/N_3 ratios were in good agreement with the actual stoichiometry of the sample. In the case of AN, the hygroscopic nature of the compound affected the stoichiometric ratios.

We had also performed ns and fs LIBS on other HEMs such as RDX, HMX, and NTO. Figure 1 shows typical fs LIBS spectra of NTO, TNT, RDX, PETN, and HMX pellets

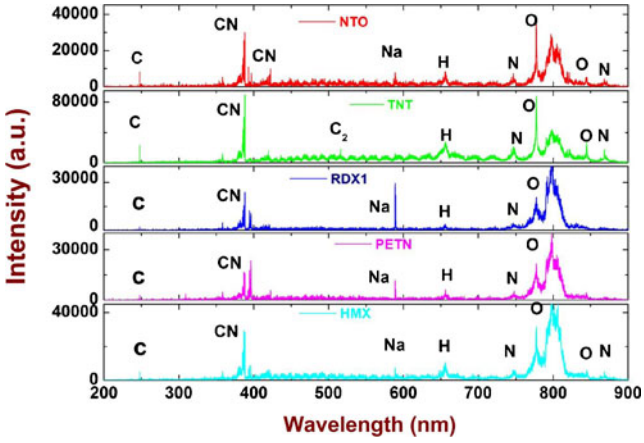

Figure 1. Femtosecond LIBS spectra of NTO, TNT, RDX, PETN, and HMX recorded with similar experimental conditions. A gate width of 800 ns and a gate delay of 100 ns were used to collect the spectra. Pure pellets of these molecules were prepared and used.

recorded with a gate delay of 100 ns and a gate width of 100 ns. It is evident that all the spectra look similar. From our detailed experimental data analysis we have observed that the molecular behaviour in the LIBS spectra of high-energy materials such as RDX and HMX obtained with different pulses (ns and fs) was different [20]. The main characteristics observed from both the spectra were: (a) the ratio of CN peaks (388.28 nm, 387.08 nm, 386.16 nm) to C peak (247.82 nm), recorded with similar fluences, was discovered to be stronger in the fs case, (b) CN molecular species existed for a longer time when formed with ns pulses compared to fs pulses, (c) intensity of all the elemental peaks decreased very fast in fs LIBS spectra compared to ns LIBS spectra. After successful initial screening, one could further develop powerful algorithms/schemes [20] for the fool proof discrimination of hazardous materials. Successful algorithms were indeed developed recently by our group to discriminate pharmaceutical tablets [20].

Fs LIBS spectra were recorded for RDX, NTO, and TNT in three different atmospheres of air, argon, and nitrogen [22]. The CN violet band for $\Delta v = 0$ transitions in the spectral range of 388–385 nm was observed to be strong in nitrogen and air atmospheres compared to argon. CN/C and CN/N ratios exhibited higher values in nitrogen and then decreased for data recorded in air atmosphere and further reduction was observed in the data recorded in argon atmosphere. Since the amount of surrounding nitrogen content reduced (nitrogen to air to argon atmospheres), the ratios were observed to be decreasing. The chemical reactions involved in the formation of CN, which were due to C_2 and C combining with molecular N_2 leading to the formation of CN, were dominant in nitrogen and air atmospheres because of the presence of a large amount of nitrogen. In argon atmosphere, the nitrogen species available in the plasma only would give rise to CN molecule formation implying lower probability in this atmosphere. Temporal evolution of C, CN peaks intensity was studied in all three different atmospheres [22]. The quantitative magnitudes of these elemental and molecular ratios could lead to primary discrimination of these samples. Further experiments are in progress to identify mechanisms [23–25] for the discrimination of HEMs.

2.2 *Fs LDW studies*

Using the LDW technique we had successfully achieved micro-/nanostructures on the surface and beneath the surface with fs laser micromachining in polymers such as polymethyl methcrylate (PMMA), polydimethylsiloxane (PDMS), polystyrene (PS), and polyvinyl alcohol (PVA) [35–43]. Fabrication of microstructures, complex structures, voids, gratings, and microcraters were investigated at various focussing conditions and laser parameters. Some of the spectroscopic tools used for characterizing these structures were transmission, emission, excitation, confocal micro-Raman, and electron spin resonance (ESR) techniques in the context of the formation of free radicals, optical centres and paramagnetic centres. The main reason for the observation of emission when excited at different wavelengths was the formation of optical centres in the fs laser-irradiated regions of polymers [39,40]. Existence of paramagnetic centres was confirmed through the ESR analysis in PMMA, PDMS, and PS. The observation of free radicals (including optical centres and paramagnetic centres) leading to the redistribution of elements was confirmed from the energy-dispersive X-ray absorption spectroscopy (EDXAS) analysis [36]. Raman spectral analysis of these polymers indicated bond scission, disappearance,

and softening due to the huge stress induced in the polymers [37]. Figure 2a depicts field emission scanning electron microscope (FESEM) image of a typical single surface structure in PMMA (∼30 μJ, 0.5 mm/s) while figure 2b shows a fabricated microstructure on the surface of the PS film achieved with experimental parameters of 1 mm/s, 635 nJ. Figure 2c illustrates a microstructure on the surface of the bulk PVA fabricated at 1 mm/s speed with ∼10 μJ energy. Figure 2d shows a large area two-dimensional PMMA surface grating. Such surface and subsurface structures find straight applications in microfluidics and photonics.

Various microstructures including optical waveguides were also inscribed in the bulk of different glasses. Microgratings were inscribed in fused silica, Foturan, GE124, zinc tellurite, and Baccarat glasses [43,44]. The change in refractive index was estimated to be $\sim 10^{-3}$ from the diffraction efficiency measurements. By utilizing a slit before the microscope objective, a structure of ∼750 nm width (less than diffraction limit) was achieved in Baccarat glass. Wave guiding was demonstrated in the subsurface structures written in Baccarat glasses achieved using a rectangular slit. The lowest estimated propagation loss accomplished in one of the waveguides was ∼0.9 dB/cm [44]. The future development of fs LDW technique has two motives. First, the advantages of femtosecond pulses in creating microfluidic channels towards lab-on-a-chip (LOC) applications are well established. Our attempts are in the direction of creating inexpensive LOC devices for detecting explosives. Second, fs pulses recently were used to produce controlled patterns of internal

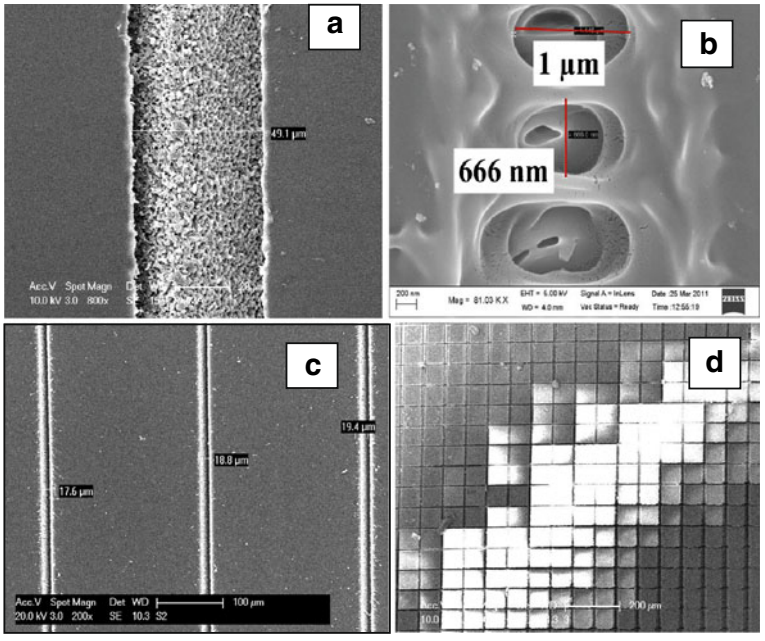

Figure 2. **(a)** Field emission scanning electron microscope (FESEM) image of PMMA single surface microstructure, **(b)** microstructures on the surface of PS film fabricated at 1 mm/s speed, 635 nJ, **(c)** microstructures on the surface of bulk PVA (1 mm/s, 10 μJ), and **(d)** FESEM image of typical surface 2D grating in PMMA.

voids in high explosive single crystals such as PETN, RDX, and HMX [65]. Consolidation of a large number of individual voids allowed the creation of wee-defined 2D and 3D structures. Production of such structures led to crystal damage or residual strain over 10–100 μm distances. Such studies are valuable for controlled studies of hot spot initiation in shocked explosives.

2.3 *Ns and fs ablation studies*

Fs laser ablation of bulk aluminum (Al) sample in oxygen-free liquid media such as CCl_4 and $CHCl_3$ in an open air environment led to the generation of Al nanoparticles and structure formation of both micro- and nanodimensions depend on the focussing conditions [32,33]. These structures will be useful in enhancing the Raman signal since these nanostructures can invoke surface plasmon resonances and therefore can be used for sensitive detection of HEMs. The average size of Al NPs was 20–40 nm in CCl_4 and 10–25 nm in $CHCl_3$. We had also fabricated stable silver NPs and NSs effectively through double ablation of bulk silver substrate immersed in double distilled water using $\sim$2 ps laser pulses [29]. The effects of multiple/double/single ablation on silver substrate via surface morphology studies along with average size distribution of Ag NPs were investigated. Depending on the ablation parameters, average sizes observed were 13 nm/17 nm in multiple/double ablation case and $\sim$7 nm in single ablation case. High-resolution transmission electron microscope (TEM) studies highlighted that most of the Ag NPs were spherical and polycrystalline in nature. Surface morphology of the substrates was characterized by FESEM and atomic force microscope (AFM). A different scenario was observed in the double ablation case compared to single/multiple ablation case. Double ablation resulted in cone-like NSs on the substrate with dimensions of few hundreds of nanometres while single ablation did not. Surface-enhanced Raman spectroscopic studies of adsorbed Rhodamine 6G on multiple/double ablated Ag substrates were carried out with excitation wavelengths of 532 nm, 785 nm and three orders of enhancement in Raman signal intensity was observed. Furthermore, influence of laser fluence on the fabrication of SERS active Ag substrates with double ablation was also investigated. In this case Raman spectra of adsorbed RDX molecules on ablated surfaces were recorded for 532 nm and 785 nm excitations. Enhancements up to 460 were observed from substrates fabricated at 12 J/cm^2 and 16 J/cm^2 fluences with 532 nm and 785 nm excitation wavelengths, respectively.

Raman spectra shown in figure 3 which were recorded with WITech Alpha 300 spectrometer used an excitation wavelength of 532 nm which utilized a 100$\times$ objective and beam waist at the focus was estimated to be $\sim$650 nm. Time of integration for both the spectra was 5 s. Elevation of the Raman modes of the analyte depends on the surface morphology of the laser-ablated surface to provide the excitation of localized surface plasmon resonances (LSP). To estimate the enhancement factor, Raman spectra of the ANTA (dissolved in acetonitrile) of 0.1 M (10 μL) was recorded from the Si substrate. At this concentration, the spectrum overlapped with Raman signatures on the continuum background was observed. Enhancement factors were estimated for both Ag and Cu nanostructures on the substrate. Since number of molecules in the analyte depends on concentration, a rough estimation of enhancement factor (EF) can be considered as analytical enhancement factor. Therefore, for the 1357 cm^{-1} mode EF is 10^2 since

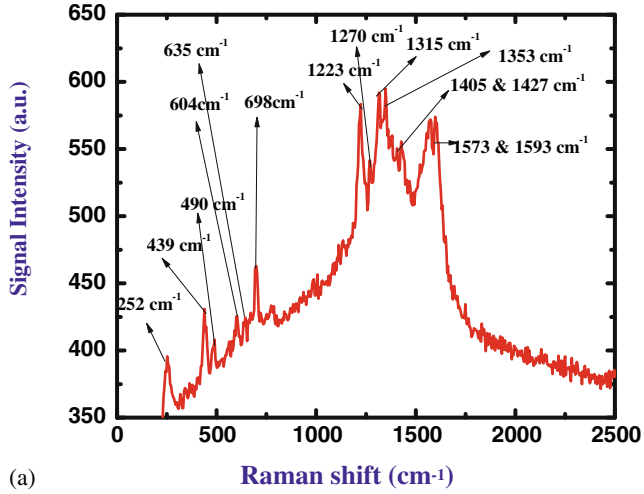

(a)

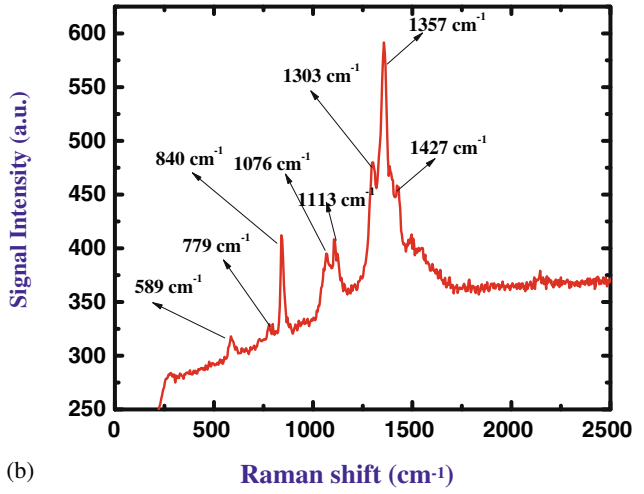

(b)

Figure 3. Raman spectra of the explosive molecules ANTA (dissolved in acetonitrile) of 5 mM concentration adsorbed on **(a)** Ag substrate ablated in chloroform with ∼2 ps laser pulses and **(b)** Cu substrate ablated in DCM with ∼2 ps laser pulses.

$C_{\text{Raman}} = 0.1$ M and $C_{\text{SERS}} = 5$ mM. Assuming 20% adsorption factor, the estimated enhancement factor will be $\sim 2 \times 10^3$ for both the cases (Ag and Cu).

$$\text{EF} = \frac{I_{\text{SERS}}}{I_{\text{Raman}}} \frac{C_{\text{Raman}}}{C_{\text{SERS}}}.$$

Figure 4 shows typical field emission scanning electron microscope (FESEM) images of the fs (∼40 fs) laser-exposed portion in Al substrate in (a)-(b) water. (a) Micrograt-ings were observed when the focus was exactly on the surface of substrate (fluence of

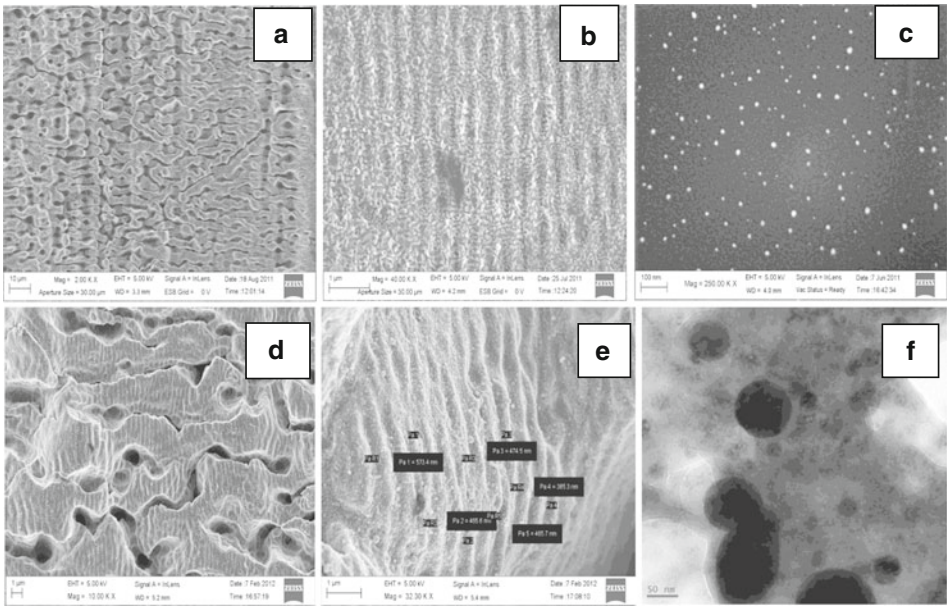

Figure 4. FESEM images of the laser-exposed Al substrate in **(a)–(b)** water. **(a)** Micrograting (20 J/cm^2), **(b)** periodic ripples observed on the Al substrate immersed in water. These ripples were observed when the focus was beyond the substrate (3 J/cm^2), **(c)** FESEM image of $CHCl_3$ colloidal solutions (20 J/cm^2) with ∼20 nm average nanoparticle size obtained at 250 μJ in the fs regime. FESEM images of the laser-exposed Cu substrate in (**d**)–(**f**) water. **(d)** (10 KX) microgratings were observed when the focus was exactly on the surface of the substrate (10 J/cm^2), **(e)** magnified image of **(d)**, showing periodic nanograting (average size of 465 nm) observed on Cu substrate immersed in water, **(f)** TEM image of water–Cu colloidal solutions (10 J/cm^2) of ∼35 nm average nanoparticle size obtained at 150 μJ in ps regime.

20 J/cm^2), (b) shows the image of the periodic ripples observed on the Al substrate immersed in water. These ripples were observed when the focus was beyond the substrate (3 J/cm^2). Figure 4c depicts the FESEM image of $CHCl_3$ colloidal solutions (20 J/cm^2). Average nanoparticle size was ∼20 nm obtained at 250 μJ in the fs regime. FESEM images of the ps (∼2 ps) laser-exposed portion in the Cu substrate in water are shown in figures 4d–4f. Figure 4d depicts microgratings which were observed when the focus was exactly on the surface of the substrate (fluence of 10 J/cm^2), (e) is the magnified image of (d), showing periodic nanograting (with average size of 465 nm) observed on the Cu substrate immersed in water. Figure 4f illustrates the TEM image of water–Cu colloidal solutions (fluence of 10 J/cm^2) with an average nanoparticle size of ∼35 nm obtained with 150 μJ in the ps regime. Our ultimate goal is to create (a) reproducible NPs and large-area (few cm^2) NSs in Al, Cu, Ag, alloys, (b) explore their SERS characteristics, and (c) obtain optimized structures for sensing different HEMs in the nanomolar concentration range.

2.4 *Ps and fs ultrafast dynamics studies*

Ultrafast excited state dynamics have been appraised of four novel corroles using picosecond (ps) and femtosecond (fs) degenerate pump–probe techniques having 800 nm and 600 nm excitation wavelengths, respectively [50]. The excitation by 800 nm photons resulted in two-photon absorption, at adequately high peak intensities, thereby facilitating the access to higher excited states (S_n). The non-radiative relaxation mechanisms from these states, reflected in the pump–probe data, consisted of biexponential decay with a slow component in the range of 54–277 ps and a faster component of 2.0–2.5 ps, limited by the pulse duration. When excited with 600 nm photons (unfocussed), photoinduced absorption resulted in populating only the first excited state S_1 and as a consequence single decay was observed in the data of all molecules studied. These lifetimes were analogous to those obtained with ps pump–probe data. The long lifetime is attributed to the non-radiative decay from S_1 state while the shorter lifetime is attributed to the internal conversion process (S_2 to S_1). Measurement of time-resolved fluorescence lifetime revealed that the radiative lifetimes were in the nanosecond regime.

Ultrafast excited state dynamics of dinaphthoporphycenes were investigated using femtosecond- and picosecond-degenerate pump–probe techniques at 600 nm and 800 nm, respectively [49]. Fs pump–probe data indicated photoinduced absorption at 600 nm resulting from two-photon/single photon excitation whereas ps pump–probe data demonstrated photobleaching which was a consequence of three-photon absorption. The fastest lifetimes (100–120 fs) observed are attributed to the intramolecular vibrational relaxation, the slower ones (1–3 ps) to internal conversion, and the slowest components (7–10 ps) to non-radiative decay back to ground state.

Our aim is to develop pump–probe techniques to evaluate the vibrational dynamics in HEMs. For example, nitromethane (CH_3NO_2) is the simplest member of a series of energetic nitrocompounds that are of great interest to the HEMs community. Nitromethane has 15 vibrational degrees of freedom. If a particular mode of the molecule is excited, the de-excitation follows two ways: (1) energy relaxation and (2) phase relaxation. Energy relaxation is an incoherent process whereas phase relaxation is a coherent phenomenon. The energy relaxation dynamics can be obtained from anti-Stokes Raman experiments through which vibrational energy re-distribution and its time evolution mechanisms can be investigated [16]. These relaxation times and pathways play crucial roles in the process of detonation. Femtosecond laser pump–probe techniques were also utilized for understanding the mechanism of dynamics of photodissociation of HMX, RDX from excited electronic states at three wavelengths (230 nm, 228 nm, 226 nm) to monitor the time evolution of the NO product [13]. Bernstein's group [10–13] has extended efforts towards understanding the critical role of non-adiabatic couplings in the initial steps of the excited electronic state decomposition of energetic materials. These experiments provide a potentially useful methodology for accurate and predictive determination, design, and synthesis of new energetic materials.

3. Conclusions

Four different ultrashort laser–matter interaction mechanisms have been deliberated. Laser direct writing was utilized to achieve several photonic structures (including

waveguides, channels, gratings etc.) in polymers and glasses. LIBS studies using ns and fs pulses facilitated our understanding of the plasma dynamics in sub-ns regime thereby building initial strategies for the discrimination of high-energy materials. Ps and fs ablation enabled us to create nanoparticles in solution and nanostructures on the substrate when ablation was performed in liquids. Ps and fs pump–probe techniques have been established and initial results from simple molecules were obtained and these techniques will be upgraded to understand the vibrational dynamics in HEMs. Further detailed studies are necessary in this ultrafast laser–matter interaction studies to understand the underlying physical/chemical dynamics and to further improve the capabilities of HEMs detection using (a) laser-based standoff techniques [66–68], (b) ultrafast coherent anti-Stokes Raman spectroscopic techniques [69,70], and (c) LIBS techniques [71–73]. These studies are also essential to explore the shock-induced physical/chemical modifications in HEMs [74,75].

Acknowledgements

The author acknowledges the support and encouragement of Prof. D Narayana Rao, Prof. Surya P Tewari, Dr P. Prem Kiran, Dr G Manoj Kumar, Dr P K Panda, and Dr L Giribabu. The author also gratefully acknowledges the contribution of various students including K C Vishnubhatla, R S S Kumar, K L N Deepak, S Sreedhar, D Swain, P T Anusha, G Krishna Podagatlapalli, S Hamad, E Nageswara Rao, and T Shuvan Prashant. Author also acknowledges DRDO for financial support.

References

[1] U Keller, *Nature* **424**, 831 (2003)
[2] G Cerullo and S De Silvestri, *Rev. Sci. Instrum.* **74**, 1 (2003)
[3] J R Vázquez de Aldana, P Moreno and L Roso, *Opt. Mater.* **34**, 572 (2012)
[4] E G Gamaly, *Phys. Rep.* **508**, 91 (2011)
[5] G Ravindra Kumar, *Pramana – J. Phys.* **73**, 113 (2009)
[6] M Dantus and V V Lozovoy, *Chem. Rev.* **104**, 1813 (2004)
[7] A Vogel, J Noack, G Huttman and G Paltauf, *Appl. Phys. B* **81**, 1015 (2005)
[8] C B Schaffer, A Brodeur and E Mazur, *Meas. Sci. Technol.* **12**, 1784 (2001)
[9] M R Leahy-Hoppa, J Miragliotta, R Osiander, J Burnett, Y Dikmelik, C McEnnis and J B Spicer, *Sensors* **10**, 4342 (2010)
[10] A Bhattacharya, Y Guo and E R Bernstein, *Acc. Chem. Res.* **43(12)**, 1476 (2010)
[11] A Bhattacharya, Y Guo and E R Bernstein, *J. Chem. Phys.* **136**, 024321 (2012)
[12] Y Guo, A Bhattacharya and E R Bernstein, *J. Phys. Chem. A* **115**, 9349 (2011)
[13] M Greenfield, Y Q Guo and E R Bernstein, *Chem. Phys. Lett.* **430**, 277 (2006)
[14] A Strachan, A C T van Duin, D Chakraborty, S Dasgupta and W A Goddard III, *Phys. Rev. Lett.* **91(9)**, 098301 (2003)
[15] R W Conner and Dana D Dlott, *J. Phys. Chem. C* **116**, 14737 (2012)
[16] S Shigeto, Y Pang, Y Fang and Dana D Dlott, *J. Phys. Chem. B* **112**, 232 (2008)
[17] Dana D Dlott, *Annu. Rev. Phys. Chem.* **50**, 251 (1999)
[18] Dana D Dlott, *Annu. Rev. Phys. Chem.* **62**, 575 (2011)
[19] S Sreedhar, M Ashwin Kumar, G Manoj Kumar, P Prem Kiran, Surya P Tewari and S Venugopal Rao, *ISRN Optics*, Article ID 631504, 2012, DOI: 10.5402/2012/631504

[20] M Ashwin Kumar, S Sreedhar, I Barman, N C Dingari, S Venugopal Rao, P Prem Kiran, Surya P Tewari and G Manoj Kumar, *Talanta* **87**, 53 (2011)
[21] S Sreedhar, G Manoj Kumar, M Ashwin Kumar, P Prem Kiran, Surya P Tewari and S Venugopal Rao, *Spectrochim. Acta* **79–80**, 31 (2012)
[22] S Sreedhar, E Nageswara Rao, G Manoj Kumar, Surya P Tewari and S Venugopal Rao, *Spectrochim. Acta* **87**, 121 (2013), http://dx.doi.org/10.1016/j.sab.2013.05.006
[23] E Nageswara Rao, S Sreedhar, G Manoj Kumar, Surya P Tewari and S Venugopal Rao, in: *Chemical, biological, radiological, nuclear, and explosives (CBRNE) sensing XIV* edited by A W Fountain, *Proc. SPIE* **8710**, 87101O (2013)
[24] S Sreedhar, E Nageswara Rao, G Manoj Kumar, Surya P Tewari and S Venugopal Rao, in: *Chemical, biological, radiological, nuclear, and explosives (CBRNE) sensing XIV* edited by A W Fountain, *Proc. SPIE* **8710**, 871012 (2013)
[25] S Sreedhar, E Nageswara Rao, G Manoj Kumar, Surya P Tewari and S Venugopal Rao, *Next-generation spectroscopic technologies VI edited* by M A Druy and R A Crocombe, *Proc. SPIE* **8726**, 87260H (2013)
[26] D W Hahn and N Omenetto, *Appl. Spectrosc.* **64**, 335A (2010)
[27] D W Hahn and N Omenetto, *Appl. Spectrosc.* **66**, 347 (2012)
[28] M Civis, S Civis, K Sovova, K Dryahina, P Spanel and M Kyncl, *Anal. Chem.* **83**, 1069 (2011)
[29] G Krishna Podagatlapalli, S Hamad, S Sreedhar, Surya P Tewari and S Venugopal Rao, *Chem. Phys. Lett.* **530**, 93 (2012)
[30] G Krishna Podagatlapalli, S Hamad, S Sreedhar, Surya P Tewari and S Venugopal Rao, *J. Appl. Phys.* **113**, 073106 (2013)
[31] S Hamad, G Krishna Podagatlapalli, Surya P Tewari and S Venugopal Rao, *J. Phys. D: Appl. Phys.* **46**, 485501 (2013)
[32] S Hamad, G Krishna Podagatlapalli, Surya P Tewari and S Venugopal Rao, *Proc. SPIE* **8245**, 82450L (2012)
[33] S Hamad, G K Podagatlapalli, A Hussain, N Ahmed, S Sreedhar, Surya P Tewari and S Venugopal Rao, in *International Conference on Fibre Optics and Photonics*, OSA Technical Digest (online) (Optical Society of America, 2012), MPo.31. http://www.opticsinfobase.org/abstract.cfm?URI=Photonics-2012-MPo.31
[34] R R Gattass and E Mazur, *Nat. Phot.* **2**, 219 (2008)
[35] K L N Deepak, D Narayana Rao and S Venugopal Rao, *Laser-induced damage in optical materials* edited by G J Exarhos, V E Gruzdev, J A Menapace, D Ristau and M J Soileau, *Proc. SPIE* **8530**, 853004 (2012)
[36] K L N Deepak, S Venugopal Rao and D Narayana Rao, *Opt. Eng.* **51**, 073402 (2012)
[37] K L N Deepak, S Venugopal Rao and D Narayana Rao, *Laser pulses* edited by Igor Peshko (InTech Publishers, Croatia, 2012) pp. 277–294, ISBN 979-953-307-845-7
[38] K L N Deepak, R Kuladeep, S Venugopal Rao and D Narayana Rao, *Rad. Effects Defects Solids* **167(2)**, 88 (2012)
[39] K L N Deepak, D Narayana Rao and S Venugopal Rao, *Appl. Opt.* **49(13)**, 2475 (2010)
[40] K L N Deepak, S Venugopal Rao and D Narayana Rao, *Appl. Surf. Sci.* **257**, 9299 (2011)
[41] K L N Deepak, R Kuladeep, V Praveen Kumar, S Venugopal Rao and D Narayana Rao, *Opt. Commun.* **284(12)**, 3074 (2011)
[42] K L N Deepak, S Venugopal Rao and D Narayana Rao, *Chem. Phys. Lett.* **503**, 57 (2011)
[43] K L N Deepak, S Venugopal Rao and D Narayana Rao, *Pramana – J. Phys.* **75(6)**, 1221 (2010)
[44] K L N Deepak, S Venugopal Rao and D Narayana Rao, *Proc. SPIE* **8190**, 81900R (2011)
[45] K C Vishnubhatla, S Venugopal Rao, R Sai Santosh Kumar, M Ferrari and D Narayana Rao, *Opt. Commun.* **282**, 4537 (2009)
[46] K C Vishnubhatla, S Venugopal Rao, R Sai Santosh Kumar, R Osellame, S N B Bhaktha, S Turrell, A Chiappini, A Chiasera, M Ferrari, M Mattarelli, M Montagna, R Ramponi, G C Righini and D Narayana Rao, *J. Phys. D.: Appl. Phys.* **42**, 205106 (2009)

[47] S Venugopal Rao, D Swain and Surya P Tewari, in *Organic photonic materials and devices XII* edited by R L Nelson, F Kajzar and T Kaino, *Proc. SPIE* **7599**, 75991P (2010)
[48] D Swain, A Rana, P K Panda and S Venugopal Rao, *Proc. SPIE* **8258**, 82581B (2012)
[49] D Swain, P T Anusha, T S Prashant, T Sarma, P K Panda, S P Tewari and S Venugopal Rao, *Appl. Phys. Lett.* **100**, 141109 (2012)
[50] P T Anusha, D Swain, S Hamad, L Giribabu, T S Prashant, Surya P Tewari and S Venugopal Rao, *J. Phys. Chem. C* **116**, 17828 (2012)
[51] S Venugopal Rao, P T Anusha and Surya P Tewari, in *International Conference on Fibre Optics and Photonics*, OSA Technical Digest (online) (Optical Society of America, 2012), paper TPo.5. http://www.opticsinfobase.org/abstract.cfm?URI=Photonics-2012-TPo.5
[52] S Venugopal Rao, T Shuvan Prashant, D Swain, T Sarma, P K Panda and S P Tewari, *Chem. Phys. Lett.* **514**, 98 (2011)
[53] T Sarma, Pradeepta K Panda, P T Anusha and S Venugopal Rao, *Org. Lett.* **13(2)**, 188 (2011)
[54] R S S Kumar, S Venugopal Rao, L Giribabu and D Narayana Rao, *Opt. Mater.* **31**, 1042 (2009)
[55] S Venugopal Rao, N Venkatram, L Giribabu and D Narayana Rao, *J. Appl. Phys.* **105**, 053109 (2009)
[56] N Venkatram, L Giribabu, D Narayana Rao and S Venugopal Rao, *Chem. Phys. Lett.* **464**, 211 (2008)
[57] R S S Kumar, S Venugopal Rao, L Giribabu and D Narayana Rao, *Chem. Phys. Lett.* **447**, 274 (2007)
[58] N Venkatram, L Giribabu, D Narayana Rao and S Venugopal Rao, *Appl. Phys. B* **91**, 149 (2008)
[59] P T Anusha, L Giribabu, Surya P Tewari and S Venugopal Rao, *Mater. Lett.* **64**, 1915 (2010)
[60] S Venugopal Rao, P T Anusha, L Giribabu and Surya P Tewari, *Pramana – J. Phys.* **75(5)**, 1017 (2010)
[61] D Swain, R Singh, V K Singh, N V Krishna, L Giribabu and S Venugopal Rao, *J. Mater. Chem. C* (in press) (2014), DOI: 10.1039/C3TC31640H
[62] S Venugopal Rao, *J. Mod. Opt.* **58(12)**, 1024 (2011)
[63] S Hamad, Surya P Tewari, L Giribabu and S Venugopal Rao, *J. Porphy. Phth.* **16(1)**, 140 (2012)
[64] D Swain, P T Anusha, T Sarma, P K Panda and S Venugopal Rao, *Chem. Phys. Lett.* **580**, 73 (2013)
[65] S D McGrane, A Grieco, K J Ramos, D E Hooks and D S Moore, *J. Appl. Phys.* **105**, 073505 (2009)
[66] S Wallin, A Pettersson, H Ostmark and A Hobro, *Anal. Bioanal. Chem.* **395**, 259 (2009)
[67] B Wen and H Eilers, *Appl. Phys. B* **106**, 473 (2012)
[68] J S Caygill, F Davis and S P J Higson, *Talanta* **88**, 14 (2012)
[69] M Bremer, P Wrzesinski, N Butcher, V V Lozovoy and M Dantus, *Appl. Phys. Lett.* **99**, 101109 (2011)
[70] H Li, D A Harris, B Xu, P J Wrzesinski, V V Lozovoy and M Dantus, *Opt. Exp.* **16**, 5499 (2008)
[71] J L Gottfried, F C De Lucia Jr, C A Munson and A W Miziolek, *J. Anal. At. Spectrom.* **23**, 205 (2008)
[72] J L Gottfried, F C De Lucia Jr, C A Munson and A W Miziolek, *Anal. Bioanal. Chem.* **395**, 283 (2009)
[73] P Lucena, A Doña, L M Tobaria and J J Laserna, *Spectrochim. Acta Part B* **66**, 12 (2011)
[74] J E Patterson, Z A Dreger, M Miao and Y M Gupta, *J. Phys. Chem. A* **112**, 7374 (2008)
[75] N C Dang, Z A Dreger, Y M Gupta and D E Hooks, *J. Phys. Chem. A* **114(43)**, 11560 (2010)